ARTICLE

Genetic variants beyond amyloid and tau associated with cognitive decline

A cohort study

Hang-Rai Kim, MD, Taeyeop Lee, MD, Jung Kyoon Choi, PhD, and Yong Jeong, MD, for the Alzheimer's Disease Neuroimaging Initiative

Correspondence
Dr. Jeong
yong@kaist.ac.kr

Neurology® 2020;95:e2366-e2377. doi:10.1212/WNL.0000000000010724

Abstract

Objective

To identify single nucleotide polymorphisms (SNPs) associated with cognitive decline independent of β-amyloid (Aβ) and tau pathology in Alzheimer disease (AD).

Methods

Discovery and replication datasets consisting of 414 individuals (94 cognitively normal control [CN], 185 with mild cognitive impairment [MCI], and 135 with AD) and 72 individuals (22 CN, 39 with MCI, and 11 with AD), respectively, were obtained from the Alzheimer's Disease Neuroimaging Initiative database. Genome-wide association analysis was conducted to identify SNPs associated with individual cognitive function (measured with the Mini-Mental State Examination and Alzheimer's Disease Assessment Scale–Cognitive Subscale) while controlling for the level of Aβ and tau (measured as CSF phosphorylated-tau/$A\beta_{1\text{-}42}$). Gene ontology analysis was performed on SNP-associated genes.

Results

We identified 1 significant (rs55906536, $\beta = -1.91$, standard error 0.34, $p = 4.07 \times 10^{-8}$) and 4 suggestive variants on chromosome 6 that were associated with poorer cognitive function. Congruent results were found in the replication data. A structural equation model showed that the identified SNP deteriorated cognitive function partially through cortical thinning of the brain in a region-specific manner. Furthermore, a bioinformatics analysis showed that the identified SNPs were associated with genes related to glutathione metabolism.

Conclusions

In this study, we identified SNPs related to cognitive decline in a manner that could not be explained by Aβ and tau levels. Our findings provide insight into the complexity of AD pathogenesis and support the growing literature on the role of glutathione in AD.

From the Graduate School of Medical Science & Engineering (H.-R.K., T.L., Y.J.), KAIST Institute for Health Science and Technology (H.-R.K., Y.J.), and Department of Bio and Brain Engineering (J.K.C., Y.J.), KAIST, Daejeon, Republic of Korea.

Go to Neurology.org/N for full disclosures. Funding information and disclosures deemed relevant by the authors, if any, are provided at the end of the article.

Data used in preparation of this article were obtained from the Alzheimer's Disease Neuroimaging Initiative (ADNI) database (adni.loni.usc.edu). As such, the investigators within the ADNI contributed to the design and implementation of ADNI and/or provided data but did not participate in analysis or writing of this report. A complete listing of ADNI investigators can be found in the coinvestigators list at links.lww.com/WNL/B248.

Glossary

Aβ = β-amyloid; **AD** = Alzheimer disease; **ADAS-cog** = Alzheimer's Disease Assessment Scale–Cognitive Subscale; **ADNI** = Alzheimer's Disease Neuroimaging Initiative; **CFI** = comparative fit index; **cis-eQTL** = cis-expression quantitative trait loci; **DAB1** = disabled-1; **Hi-C** = high-throughput chromosome conformation capture; **MAF** = minor allele frequency; **MCI** = mild cognitive impairment; **MMSE** = Mini-Mental State Examination; **MoCA** = Montreal Cognitive Assessment; **p-tau** = phosphorylated tau; **PC** = principal component; **RMSEA** = root mean square error of approximation; **ROS** = reactive oxygen species; **SEM** = structural equation modeling; **SNP** = single nucleotide polymorphism.

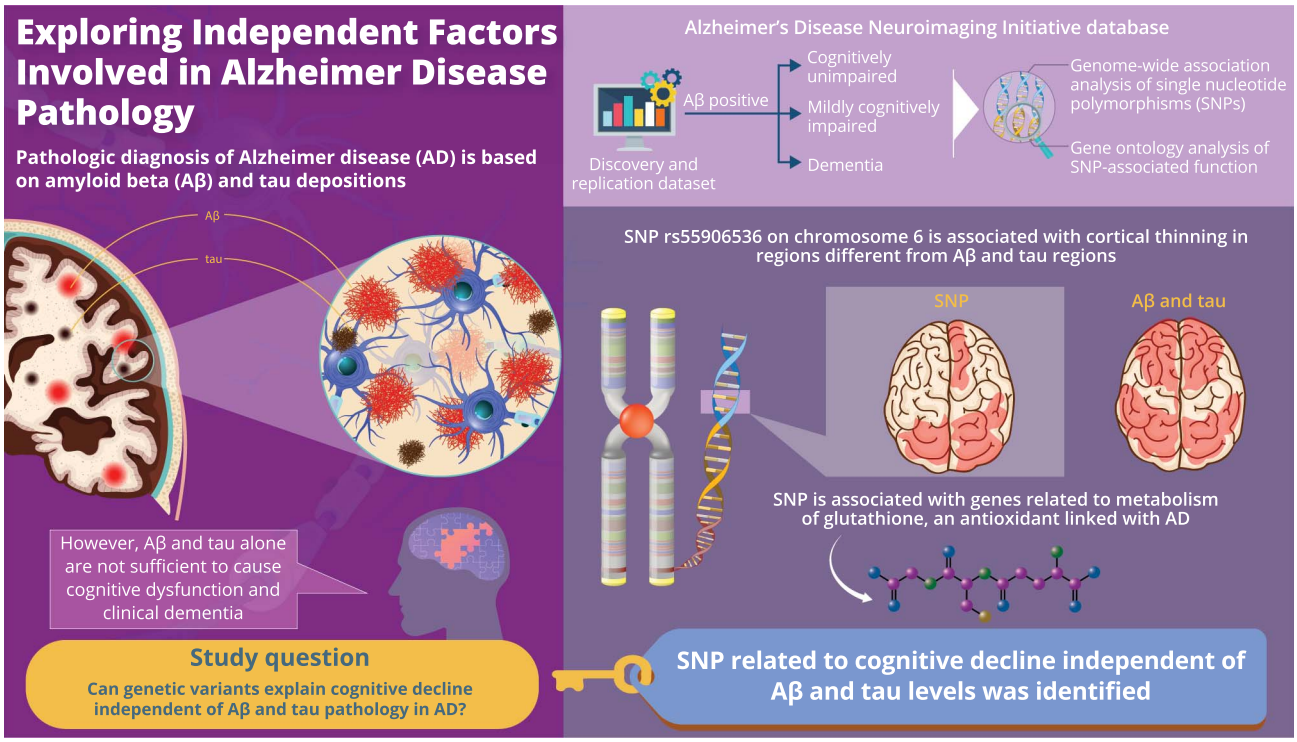

doi:10.1212/WNL.0000000000010724

Neurology®

Alzheimer's disease (AD) is characterized by accumulation of 2 key pathogenic proteins, β-amyloid (Aβ) and tau in the brain. Although pathogenic roles of these proteins have been demonstrated in a number of studies,[1,2] it is now clear that AD is a complex multifactorial disease and that Aβ and tau cannot account for all aspects of AD.[3,4] It has previously been reported that 30% to 40% of cognitively normal individuals showed an accumulation of Aβ and tau in the brain.[5,6] Furthermore, although tau accumulation showed a higher association with cognitive dysfunction than Aβ did, both pathogenic proteins demonstrated a weak to moderate association with the degree of cognitive function.[7,8] These results indicate that Aβ and tau depositions are required for the pathologic diagnosis of AD but by themselves are not sufficient to cause cognitive dysfunction and clinical dementia. Similarly, repeated failures of clinical trials of anti-Aβ therapies suggest that there may be pathogenic protein-independent factors in AD pathogenesis.[9–11]

In recent years, genome-wide association studies have discovered numerous genetic risk variants for AD[12] using Aβ and tau measured either in CSF or PET as the endophenotype. However, until now, AD studies have not assessed the genetic risk variants for cognitive deterioration, which remains unexplained by Aβ and tau accumulation. Here, we conducted a genome-wide association analysis to identify genetic variants that explain individual cognitive function independently of Aβ and tau levels in individuals with positive Aβ pathology. Considering the highly complex multifactorial mechanisms of AD, we expect that identification of such variants will help elucidate novel pathways contributing to cognitive deterioration that expand beyond processes associated with Aβ and tau.

Methods

Standard protocol approvals, registration, and patient consents

The study protocol was approved by the institutional review board of each participating Alzheimer's Disease Neuroimaging Initiative (ADNI) site (adni.loni.usc.edu/wp-content/uploads/how_to_apply/ADNI_Acknowledgement_List.pdf), and participants gave written informed consent at the time of enrollment.

Figure 1 Flowchart showing sequence of (A) participant selection and (B) analysis steps

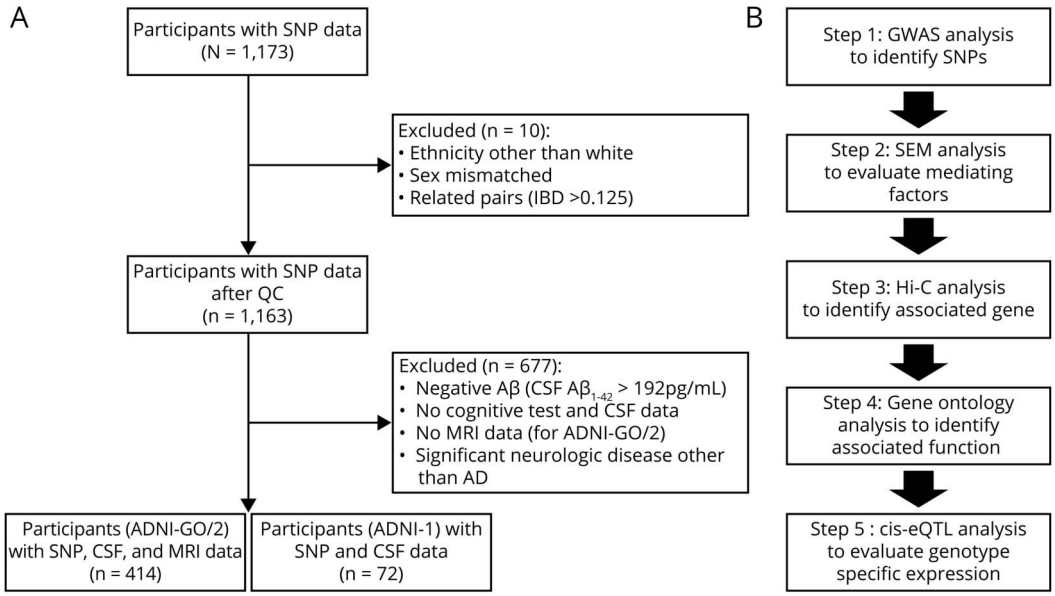

Aβ = β-amyloid; AD = Alzheimer disease; ADNI = Alzheimer's Disease Neuroimaging Initiative; cis-eQTL = cis-expression quantitative trait loci; GWAS = genome-wide association study; Hi-C = high-throughput chromosome conformation capture; IBD = identify by descent; QC = quality control; SEM = structural equation model; SNP = single nucleotide polymorphism.

Participants

Data used in the preparation of this article were obtained from the ADNI database (adni.loni.usc.edu). The ADNI was launched in 2003 as a public-private partnership led by principal investigator Michael W. Weiner, MD. The primary goal of ADNI has been to test whether serial MRI, PET, other biological markers, and clinical and neuropsychological assessment can be combined to measure the progression of mild cognitive impairment (MCI) and early AD. In the primary analysis, we used data from individuals enrolled in the ADNI-GO/2 dataset with available genetic, T1-weighted MRI, and CSF data. We included individuals who either were cognitively normal controls or had MCI or AD and with positive Aβ pathology (CSF $A\beta_{1\text{-}42}$ ≤192 pg/mL).[13] Subjects with any significant neurologic disease other than AD were excluded from the study. In the replication study, we used individuals enrolled in the ADNI-1 selected on the basis of the same inclusion and exclusion criteria as in the primary analysis. Cognitive performance was evaluated with the Mini-Mental State Examination (MMSE) and Montreal Cognitive Assessment (MoCA) scores for individuals in the ADNI-GO/2 dataset and the Alzheimer's Disease Assessment Scale–Cognitive Subscale (ADAS-cog) for the ADNI-1 dataset. Detailed diagnostic criteria are described on the ADNI website (adni-info.org).

Genotyping and imputation

Genotyping data were collected with the Illumina HumanOmniExpress Beadchip and Illumina Human610-Quad BeadChip (Illumina, San Diego, CA) for the ADNI-GO/2 and ADNI-1 databases, respectively. Only single nucleotide polymorphism (SNP) markers were analyzed in this study. Details on genome-wide association study data collection are provided on the ADNI website (adni.loni.usc/edu/data-samples/genetic-data). We initially obtained all available SNP data (ADNI Omni2.5M microarray SNP data, version 2014.2.20), which include 1,173 individuals with 581,553 SNPs. We performed quality control using PLINK software (version 1.9).[14] We excluded individuals with following criteria: the individual had an ethnicity other than White; there was a sex mismatch; and in cases of related pairs (identified with identity by descent >0.125), 1 individual of each pair was randomly excluded from the study. SNPs not meeting any of the following criteria were excluded: call rate per SNP ≥95%; minor allele frequency (MAF) ≥3%; and a value of $p \geq 10^{-5}$ on the Hardy-Weinberg equilibrium test. In total, 581,553 SNPs and 1,163 individuals passed the filter and were included for imputation. We imputed these filtered SNPs using the Michigan Imputation Server[15,16] with the following setup: 1,000 Genome Project Phase 3 version 5 as the reference panel, SHAPEIT as the phasing tool, and European as the population. For postimputation quality control, we excluded SNPs with following criteria: poor imputation quality ($r^2 \leq 0.8$) and MAF ≤0.03. A total of 6,221,501 SNPs passed the filters, and the remaining participants were divided according to their respective ADNI dataset (ADNI-GO/2 and ADNI-1). Finally, 414 participants (94 cognitively normal control, 185 with MCI, and 135 with AD) for ADNI-GO/2 and 72 individuals (22 cognitively normal control, 39 with MCI, and 11 with AD) for ADNI-1 were used in the analysis. Figure 1A shows a detailed flowchart of participant selection and analysis.

Table 1 Demographics of participants

	ADNI-GO/2				ADNI-1			
	NC (n = 94)	MCI (n = 185)	AD (n = 135)	*p* Value	NC (n = 22)	MCI (n = 39)	AD (n = 11)	*p* Value
Age (SD), y	75.9 (6.5)	74.0 (6.9)	74.4 (8.2)	0.14	77.3 (3.4)	75.1 (7.2)	73.6 (6.1)	0.24
Female, n (%)	57 (60.6)	70 (37.8)	58 (43.0)	0.001[a]	31 (48.4)	16 (30.2)	6 (50.0)	
Education (SD), y	16.3 (2.3)	16.1 (2.7)	15.7 (2.5)	0.28	15.5 (3.2)	16.6 (2.9)	14.9 (2.5)	0.15
MMSE/ADAS-cog score (SD)	28.9 (1.2)	27.5 (2.1)	23.4 (2.7)	<0.0001[b]	9.3 (5.05)	18.0 (6.9)	22.8 (3.3)	<0.0001[a]
CSF $A\beta_{1\text{-}42}$ (SD), pg/mL	148.7 (25.6)	138.6 (25.6)	127.1 (20.1)	<0.0001[b]	149.7 (24.6)	137.8 (21.3)	128.1 (23.3)	0.03[c]
CSF total tau (SD), pg/mL	75.9 (36.0)	103.6 (57.3)	134.4 (60.0)	<0.0001[b]	92.2 (33.4)	114.2 (52.0)	123.4 (52.5)	0.12
CSF p-tau (SD), pg/mL	43.6 (23.1)	50.5 (25.3)	63.0 (34.2)	<0.0001[a]	38.6 (17.7)	51.9 (31.3)	42.3 (9.1)	0.13
Global cortical thickness (SD), mm	2.48 (0.12)	2.42 (0.14)	2.27 (0.17)	<0.0001[a]	2.33 (0.13)	2.28 (0.16)	2.16 (0.16)	0.017[c]

Abbreviations: Aβ = β -amyloid; AD = Alzheimer disease; ADAS-cog = Alzheimer's Disease Assessment Scale–Cognitive Subscale; ADNI = Alzheimer's Disease Neuroimaging Initiative; MCI = mild cognitive impairment; MMSE = Mini-Mental State Examination; NC = normal control; p-tau = phosphorylated tau.
The *p* values were calculated with 1-way analysis of variance or χ^2 test. Post hoc test used Bonferroni correction.
[a] NC vs MCI, NC vs AD.
[b] NC vs MCI, MCI vs AD, AD vs NC.
[c] NC vs AD.

CSF protein concentration measurements

We used CSF data collected by the University of Pennsylvania (version 2016.7.5) for both ADNI-GO/2 and ADNI-1. The levels of $A\beta_{1\text{-}42}$, total tau, and phosphorylated tau (p-tau) in the CSF were measured with a microbead-based multiplex immunoassay (INNO-BIA AlzBio3 RUO test; Fujirebio, Ghent, Belgium). Details of CSF collection are described on the ADNI website (adni.loni.usc/edu/data-samples/biospecimen-data). We used the CSF data available at the time closest to when the cognitive tests were performed (MMSE, MoCA, and ADAS-cog).

Image acquisition and preprocessing

To assess brain atrophy, we measured the cortical thickness value using T1-weighted MRI. We used summary data, generated at the University of California, San Francisco (version 2016.8.1 for ADNI-2/GO and version 2016.2.1 for ADNI-1). Cortical reconstruction and segmentation were performed with FreeSurfer (version 4.3 in ADNI-1, version 5.1 in ADNI-2), and the cortical thickness for each of the 68 Desikan-Killiany[17]–based regions of interest was calculated (surfer.nmr.mgh.harvard.edu). A detailed description of image preprocessing is provided on the ADNI website (adni.loni.usc/edu/data-samples/mri). On the basis of previous work,[18] we calculated the global cortical thickness value using the average cortical thickness values in the following 11 AD signature regions: bilateral parahippocampus, entorhinal, fusiform, transverse and inferior temporal cortex, postcentral, posterior cingulate, precuneus, superior and inferior parietal cortex, and supramarginal cortex.

Statistical analysis

Genome-wide association analysis

A linear regression model was constructed to detect the association between SNPs and MMSE score while controlling for the CSF p-tau/$A\beta_{1\text{-}42}$ ratio, age, sex, and education level. In this study, we used CSF p-tau/$A\beta_{1\text{-}42}$ to reflect individual AD pathologic burden as established in previous studies.[19,20] We also conducted a principal component (PC) analysis of each participant's SNP data and included the first 4 PCs as a covariate in the linear model. Therefore, the linear regression model was expressed as follows: MMSE score = $\beta_0 + \beta_1$ age + β_2 sex + β_3 education + β_4 PC + β_5 p-tau/$A\beta_{1\text{-}42}$ + β_6 SNP, where β represents the coefficient and SNP (additive model, 0, 1, and 2 as the number of minor alleles) represents the genotype of each marker tested. Using this model, we identified genetic variants that explained cognitive function independently of the levels of Aβ and p-tau. Reported *p* values were 2 tailed, and we defined a value of $p < 5 \times 10^{-8}$ as being statistically significant and $p < 5 \times 10^{-7}$ as being statistically suggestive according to the previous genome-wide association study.[21] We assessed genomic inflation by dividing the median of the observed χ^2 statistics from the genome-wide association analysis by the approximate median of a χ^2 distribution with 1 *df*, a value calculated to be 0.456.[22] In the replication dataset, we used the ADAS-cog score as the quantitative cognitive measure and performed the analysis for SNPs that were identified in the primary analysis. For the replication analysis, given that the effects are expected to occur in the same direction as the results from the discovery dataset, 1-tailed *p* values are reported.

Post hoc analysis

After identifying significant SNPs, we performed a hierarchical linear regression to estimate the amount of variance in cognitive function that is explained by the SNPs. Next, we stratified all participants by the presence of the SNPs and compared baseline demographics and the level of AD pathologies. We furthermore evaluated the effect of SNPs on each cognitive domain, including memory (delayed recall score), attention (sum of target detection, serial subtraction task, and digit forward and backward score), language (sum of

Figure 2 Results of genome-wide association analysis

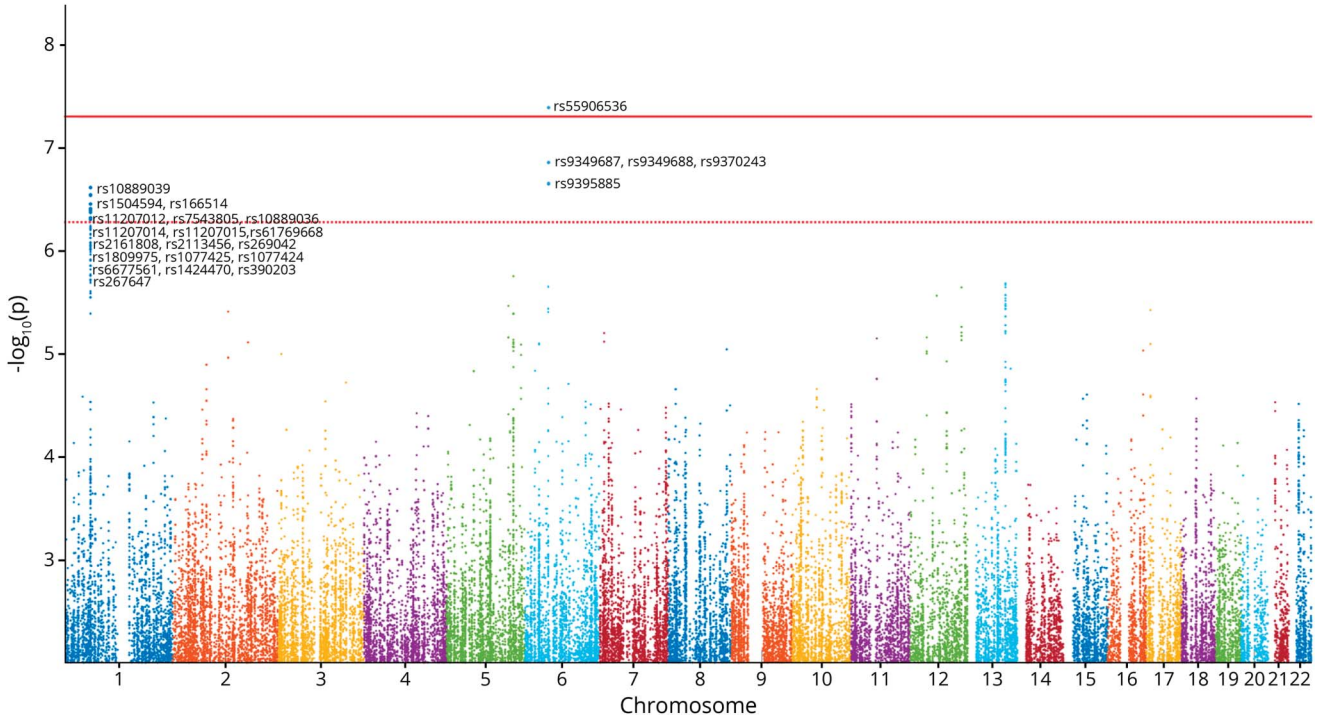

Manhattan plot showing 1 significant SNP (rs55906536) and suggestive SNPs on chromosomes 1 and 6. Solid red line indicates the genome-wide significance level ($p = 5 \times 10^{-8}$); dotted red line indicates the genome-wide suggestive level ($p = 5 \times 10^{-7}$).

3-item naming task and repetition of 2 complex sentences score), visuospatial (sum of clock-drawing task and 3D cube copy score), and executive function (sum of Trail-Making Test B task and 2-item verbal abstraction score) using MoCA subitem scores.[23] We used MATLAB (MathWorks 2014b, Natick, MA) for the above statistical analyses and result visualization.

Structural equation modeling

Next, to evaluate mediating factors between identified SNPs and cognitive decline, we performed structural equation modeling (SEM). We first built a model in which SNPs have direct and indirect paths to cognitive decline through all possible mediators, including age, sex, education, CSF p-tau/$A\beta_{1\text{-}42}$, and the global cortical thickness value. Using the biomarker model of AD,[24] we also derived an indirect path between CSF p-tau/$A\beta_{1\text{-}42}$ to cognitive decline through the global cortical thickness value (figure e-1A, data available from Dryad). After path coefficients were derived, paths were thresholded by eliminating paths with values of $p > 0.05$ to achieve a more parsimonious model. Path elimination was monitored via successive improvements of the comparative fit index (CFI) and root mean square error of approximation (RMSEA). Good model fit was assessed as a CFI of >0.90[25] and an RMSEA of >0.06 or 0.05.[26] The final model fit was bootstrapped for 500 replications, and the 95% confidence intervals of the path parameters of the final model were estimated. Using the final model, we performed SEM with 68 regional cortical thickness values to assess which regional cortical thickness changes were responsible for the cognitive decline in individuals with SNPs. SEM was conducted with AMOS software (SPSS, Chicago, IL).[27]

High-throughput chromosome conformation capture

We evaluated genes associated with identified SNPs using available high-throughput chromosome conformation capture (Hi-C) data on the hippocampus and dorsolateral prefrontal cortex (kobic.kr/3div).[28] Specifically, we identified the transcription start site of a gene that exhibited long-range chromatin interactions with the bin (5 kb in size) harboring the SNPs. We considered genes with a distance-normalized interaction frequency ≥2 as significantly associated.

Gene ontology analysis

To infer the biological significance of the identified genes, we performed gene set enrichment analysis using EnrichR (amp.pharm.mssm.edu/Enrichr).[29] The 3 functional categories of gene ontology (i.e., the biological process, cellular components, and molecular function) were analyzed. The ontology terms that have at least 2 genes and adjusted value of $p < 0.05$ were considered significant.

Genotype cis-expression quantitative trait loci analysis

In subsequent analyses, we evaluated the genotype-specific expression of identified SNPs in 48 human tissues using cis-

Table 2 Comparison between individuals by SNPs

	rs55906536			rs10889039		
	G/G (n = 339)	G/A or A/A (n = 75)	*p* Value	C/C (n = 108)	C/T or T/T (n = 306)	*p* Value
Age (SD), y	74.72 (6.89)	74.21 (9.11)	0.651	74.69 (7.42)	74.60 (7.32)	0.913
Female, n (%)	147 (43.4)	38 (50.7)	0.25	45 (41.7)	140 (45.8)	0.463
Education (SD), y	16.01 (2.54)	16.25 (3.03)	0.522	16.06 (2.75)	16.05 (2.59)	0.966
MMSE score (SD)	26.85 (2.94)	25.08 (3.61)	<0.0001	25.39 (3.56)	26.93 (2.88)	<0.0001
Presence of *APOE* ε4 allele, n (%)[a]	211 (62.6)	44 (60.3)	0.709	69 (63.9)	186 (61.6)	0.672
Diagnosis (NC/MCI/AD), n	86/155/98	8/30/37	0.001	18/42/48	76/143/87	0.008
Global cortical thickness (SD), mm	2.39 (0.16)	2.34 (0.20)	0.047	2.38 (0.18)	2.39 (0.16)	0.516
CSF $A\beta_{1\text{-}42}$ (SD), pg/mL	137.40 (25.4)	136.23 (24.4)	0.716	133.45 (25.51)	138.51 (25.05)	0.073
CSF total tau (SD), pg/mL	105.75 (58.67)	112.63 (55.86)	0.364	110.87 (59.43)	105.59 (57.75)	0.424
CSF p-tau/$A\beta_{1\text{-}42}$ (SD), pg/mL	0.41 (0.26)	0.37 (0.20)	0.249	0.40 (0.21)	0.41 (0.26)	0.817
CSF p-tau (SD), pg/mL	53.89 (29.94)	49.48 (24,2)	0.234	51.25 (25.49)	53.74 (30.16)	0.445
Time interval (SD), d[b]	37.08 (30.14)	34.09 (24.69)	0.424	34.76 (26.36)	37.17 (30.19)	0.462

Abbreviations: Aβ = β-amyloid; AD = Alzheimer disease; MCI = mild cognitive impairment; MMSE = Mini-Mental State Examination; NC = normal control; p-tau = phosphorylated tau.
The *p* values were calculated with the Student *t* test or χ^2 test.
[a] Subjects have ≥1 ε4 allele. *APOE* genotyping was not available for 4 subjects.
[b] Time interval between CSF and MMSE.

expression quantitative trait loci (cis-eQTL) analysis through the Genotype-Tissue Expression portal (gtexportal.org.home).[30] We reported genes with significant changes in expression in brain tissues ($p < 5 \times 10^{-8}$). An overall schematic diagram of the analyses is illustrated in figure 1B.

Data availability

The dataset that supports the conclusions from our genome-wide association analysis is available in the ADNI public database (adni.loni.usc.edu/data-samples/access-data/). Anonymized patient identification numbers and imaging, genetic, and biospecimen data are available from the ADNI database at the request of qualified researchers. Hi-C data from the hippocampus and dorsolateral prefrontal tissue are available at Gene Expression Omnibus (accession No. GSM2322543). Cis-eQTL data are available from the Genotype-Tissue Expression Project (gtexportal.org/home/).

Results

Description of participants

Table 1 shows the baseline demographics for the 2 datasets. As expected, patients with MCI and AD performed worse on the cognitive performance and showed higher levels of CSF p-tau and lower level of CSF $A\beta_{1\text{-}42}$ and global cortical thickness compared to cognitively normal individuals. The mean time intervals from CSF to MMSE, MoCA, and ADAS-cog were 36.4 (SD 29.2), 20.7 (SD 35.8), and 10.9 (SD 20.7) days, respectively.

Genome-wide association analysis

Genome-wide association analysis identified 1 significant (rs55906536, β = −1.91, standard error 0.34, $p = 4.07 \times 10^{-8}$), 4 suggestive variants on chromosome 6, and 19 suggestive variants on chromosome 1 (figure 2 and table e-1, data available from Dryad). A quantile-quantile plot of *p* values revealed no genomic inflation (λ = 0.98). In the replication analysis, we again observed a significant association for all 24 SNPs with the direction of the effect opposite to the findings from the discovery data (table e-1, data available from Dryad). The direction of the effect was expected because higher ADAS-cog score suggests poorer cognitive function,[31] which contrasts with MMSE and MoCA, for which lower scores indicate poorer cognitive function. Identified SNPs on each chromosome showed high linkage disequilibrium ($r^2 > 0.8$) with each other (figure e-1, data available from Dryad). Therefore, we selected rs55906536, which showed peak *p* value, for the post hoc analysis. We also performed the analysis for rs10889039, which showed peak *p* value among identified SNPs at chromosome 1.

Post hoc analysis

In the hierarchical linear regression analysis, while incorporating p-tau/$A\beta_{1\text{-}42}$ into the model explained an additional 7% of the total variance of individual cognitive function, incorporating SNPs into the model explained the additional 5% of the total variance (table e-2, data available from Dryad). When we incorporated the number of the *APOE* ε4 allele as a covariate in the model, the effect remained significant for rs55906536 (β = −1.93, standard error 0.34, $p = 4.63 \times 10^{-8}$)

Figure 3 Results of region-wide SEM

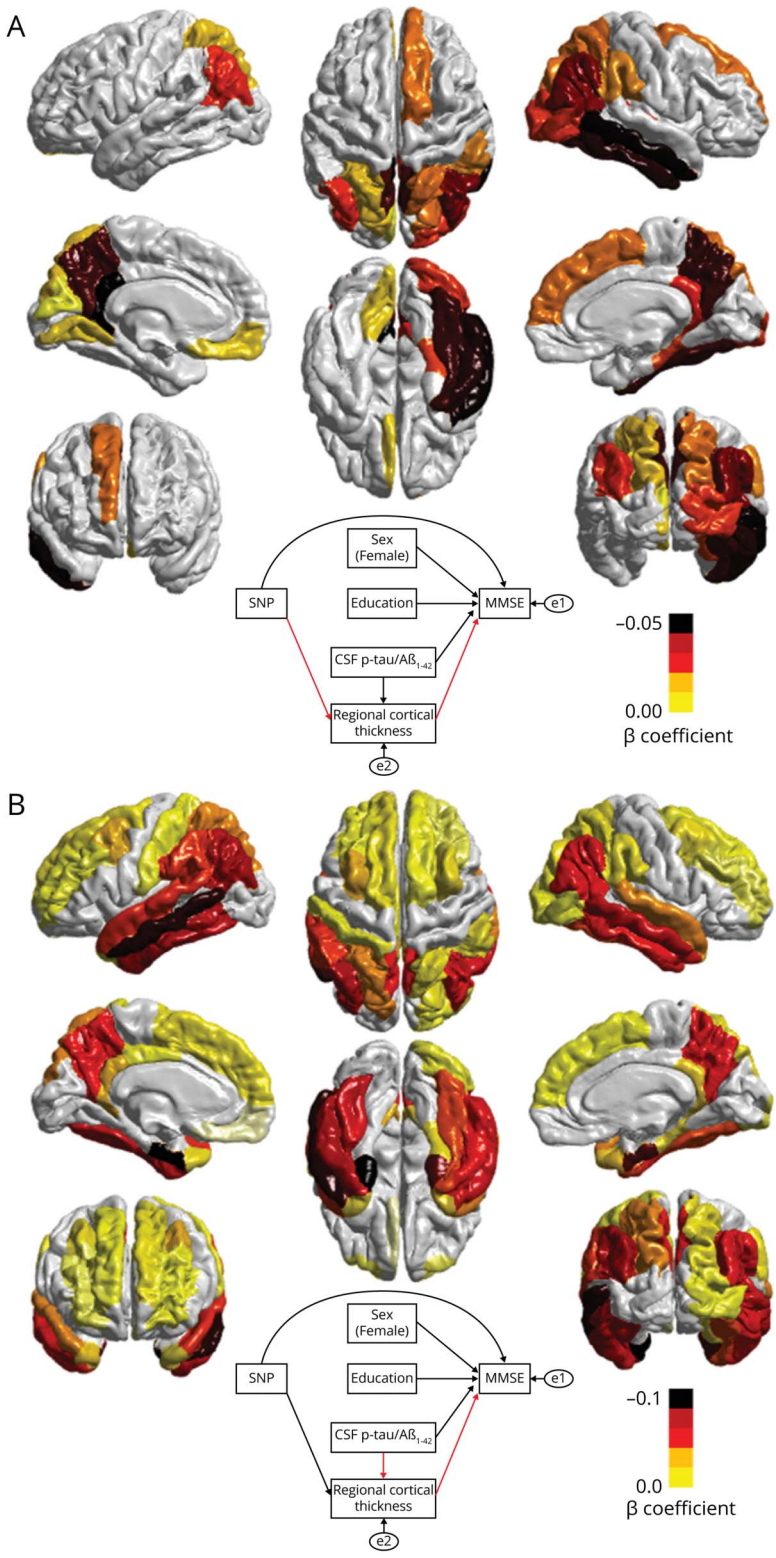

(A) Static map for indirect effect of rs55906536 through regional cortical thickness value. (B) Static map for indirect effect of CSF p-tau/A$\beta_{1\text{-}42}$ through regional cortical thickness value. Regional β coefficient was calculated with the structural equation model (SEM). Static map was thresholded by $p < 0.01$ (uncorrected). Aβ = ß - amyloid; MMSE = Mini-Mental State Examination; p-tau = phosphorylated tau; SNP = single nucleotide polymorphism.

and suggestive for rs10889039 (β = 1.02, standard error 0.19, $p = 3.42 \times 10^{-7}$). In a comparison of the demographics between individuals with and without the rs55906536 SNP, significant differences were found in MMSE scores, baseline diagnosis, and global cortical thickness values (table 2). For rs10889039, individuals with the rs10889039 SNP showed a higher MMSE score, while there was no significant difference in the level of CSF p-tau/A$\beta_{1\text{-}42}$ and global cortical thickness

Table 3 List of genes identified by Hi-C

Tissue	Bin (chromosome: position)	Distance	Distance-normalized interaction frequency	Gene
rs55906536				
Hippocampus	chr6:52535000–52540000	1205000	3.06	*TMEM14A*
Dorsolateral prefrontal cortex	chr6:53200000–53205000	540000	6.23	*RPS16P5*
Hippocampus	chr6:53860000–53865000	120000	2.31	*MLIP-IT1*
Dorsolateral prefrontal cortex	chr6:53140000–53145000	600000	2.98	*MIR5685*
Hippocampus	chr6:52145000–52150000	1595000	2.17	*MCM3*
Dorsolateral prefrontal cortex	chr6:53655000–53660000	85000	6.49	*LRRC1*
Hippocampus	chr6:52605000–52610000	1135000	8.16	*GSTA7P*
Hippocampus	chr6:52710000–52715000	1030000	2.72	*GSTA5*
Hippocampus	chr6:52770000–52775000	970000	4.47	*GSTA3*
Dorsolateral prefrontal cortex	chr6:52625000–52630000	1115000	2.32	*GSTA2*
Dorsolateral prefrontal cortex	chr6:55190000–55195000	1450000	2.29	*GFRAL*
Dorsolateral prefrontal cortex	chr6:53010000–53015000	730000	7.88	*GCM1*
Hippocampus	chr6:52930000–52935000	810000	2.49	*FBXO9*
Dorsolateral prefrontal cortex	chr6:54710000–54715000	970000	2.72	*FAM83B*
Dorsolateral prefrontal cortex	chr6:53210000–53215000	530000	4.95	*ELOVL5*
rs10889039				
Dorsolateral prefrontal cortex	Chr1:59250000–59255000	1425000	4.14	*LOC100131060*
Dorsolateral prefrontal cortex	Chr1:59245000–59250000	1420000	2.51	*JUN*
Hippocampus	Chr1:57320000–57325000	505000	2.23	*C8A*
Hippocampus	Chr1:59250000–59255000	1425000	2.19	*LOC100131060*
Hippocampus	Chr1:59775000–59780000	1950000	2.12	*FGGY*
Dorsolateral prefrontal cortex	Chr1:57285000–57290000	540000	2.04	*C1orf168*

Abbreviations: *C1orf168, FYB2* = FYN binding protein 2; *C8A* = complement C8 alpha chain; *ELOVL5* = elongation of very long chain fatty acids protein 5; *FAM83B* = family with sequence similarity 83 member B; *FBXO9* = F-box only protein 9; *FGGY* = *FGGY* carbohydrate kinase domain containing; *GCM1* = glial cells missing transcription factor 1; *GFRAL* = GDNF family receptor alpha-like; *GSTA2* = glutathione S-transferase A2; *GSTA3* = glutathione S-transferase A3; *GSTA5* = glutathione S-transferase A5; *GSTA7P* = glutathione S-transferase A7 pseudogene; Hi-C = high-throughput chromosome conformation capture; *LRRC1* = leucine-rich repeat containing 1; *MCM3* = minichromosome maintenance complex component 3; *MLIP-IT1* = muscular LMNA interacting protein-Intronic transcript 1; *MIR5685* = microRNA 5685; *RPS16P5* = ribosomal protein S16 pseudogene 5; *TMEM14A* = transmembrane protein 14A.

values (table 2). When we evaluated the effect of the SNP on each cognitive domain, individuals with rs55906536 showed the greatest deficit in visuospatial function (table e-3, data available from Dryad).

Structural equation modeling

In the SEM analysis of rs55906536, the initial model showed poor model fits (CFI 0.724, RMSEA 0.000). To modify the model, each path that did not reach the significance threshold was removed (SNP–CSF tau/$A\beta_{1\text{-}42}$, $p = 0.291$; SNP-education, $p = 0.383$; SNP-sex, $p = 0.310$; SNP-age, $p = 0.966$; age–MMSE score, $p = 0.890$). After removal of these paths, a new statistically significant model was created with an improved model fit (CFI 0.954, RMSEA 0.033). The final model indicated that both SNP and CSF p-tau/$A\beta_{1\text{-}42}$ ratios have direct and indirect paths to cognitive decline through decreased cortical thickness (figure e-2A, data available from Dryad). In the SEM using 68 regional cortical thickness values, SNP and CSF p-tau/$A\beta_{1\text{-}42}$ showed a distinct regional pattern. While changes in cortical thickness in the occipital and right parietal cortices were responsible for the indirect effect of SNPs on cognitive decline, wider areas, especially temporal cortices such as the entorhinal cortices, were responsible for the indirect effect of CSF p-tau/$A\beta_{1\text{-}42}$ (figure 3). In the SEM analysis of rs10889039, the initial model showed poor model fits (CFI 0.727, RMSEA 0.000). To modify the model, each path that did not reach the significance threshold was removed (SNP–CSF tau/$A\beta_{1\text{-}42}$, $p = 0.796$; SNP–global cortical thickness, $p = 0.38$; SNP-education, $p = 0.538$; SNP-sex,

Table 4 List of significant gene ontology of identified genes from rs55906536: Biological process and molecular function

Term	Overlap[a]	*P* Value[b]	Adjusted *p* value[c]	*z* Score[d]	Combined score[e]	Gene
Biological process						
Glutathione-derivative metabolic process	2/23	1.3×10^{-4}	0.0024	−2.29	20.49	*GSTA3, GSTA2*
Glutathione metabolic process	3/50	6.54×10^{-6}	4.7×10^{-4}	−1.55	18.60	*GSTA5, GSTA3, GSTA2*
Glutathione-derivative biosynthetic process	2/23	1.3×10^{-4}	0.0024	−1.72	15.43	*GSTA3, GSTA2*
Peptide metabolic process	3/105	6.1×10^{-6}	0.0022	−1.27	12.39	*GSTA5, GSTA3, GSTA2*
Organonitrogen compound biosynthetic process	3/182	3.1×10^{-4}	0.0045	−1.25	10.12	*GSTA3, ELOVL5, GSTA2*
Sulfur compound biosynthetic process	2/123	0.0037	0.039	−1.36	7.64	*GSTA3, GSTA2*
Molecular function						
Glutathione transferase activity	3/31	1.51×10^{-6}	2.72×10^{-5}	−1.98	26.54	*GSTA5, GSTA3, GSTA2*

Abbreviation: *ELOVL5* = elongation of very long chain fatty acids protein 5; *GSTA2* = glutathione S-transferase A2; *GSTA3* = glutathione S-transferase A3; *GSTA5* = glutathione S-transferase A5.
[a] Overlap between the input gene list and the gene set associated with the term.
[b] The *p* value was calculated with the Fisher exact test.
[c] Adjusted *p* value was obtained with the Benjamini-Hochberg method for corrections for multiple hypothesis testing.
[d] The *z* score was calculated for deviation from an expected rank with a modification of the Fisher exact test.
[e] Combined score was calculated as log(*p* value) × *z* score.

$p = 0.443$; SNP-age, $p = 0.749$; age–MMSE score, $p = 0.968$; sex–MMSE score, $p = 0.135$). After removal of these paths, a new statistically significant model was created with an improved model fit (CFI 0.988, RMSEA 0.05). The final model indicated that while rs10889039 has a direct path to cognitive decline, CSF p-tau/$A\beta_{1\text{-}42}$ showed both direct and indirect paths to cognitive decline through decreased cortical thickness (figure e-2B, data available from Dryad).

High-throughput chromosome conformation capture

We sought to verify the potential target regions of the identified SNPs through Hi-C data generated in hippocampal and dorsolateral prefrontal tissue. The bin including rs55906536 showed a strong interaction (distance-normalized interaction frequency >2) with bins located near the promoter region of 15 genes (table 3). With regard to rs10889039, the bin including rs10889039 showed a strong interaction (distance-normalized interaction frequency >2) with bins located near the promoter region of 5 genes (table 3).

Gene ontology

Gene ontology analysis showed that identified genes from rs55906536 were significantly enriched in biological processes, including a glutathione metabolic and biosynthetic process and a peptide, organonitrogen, and sulfur compound biosynthetic process. Molecular function analysis showed that identified genes were enriched in glutathione transferase activity (table 4). Cellular component analysis did not demonstrate any significant enrichment. However, with regard to rs10889039, the gene ontology analysis could not identify any significant enrichment of identified genes from rs10889039 in biological, molecular function, or cellular component.

Genotype cis-eQTL analysis

In the cis-eQTL analysis, no gene reached statistical significance for rs55906536 in the brain tissues. However, in the analysis of rs10889039, the minor allele (thymine) of rs10889039 was significantly associated with higher expression of the *DAB1* gene in 2 brain tissues (figure e-3, data available from Dryad).

Discussion

In this study, we identified 1 significant SNP (rs55906536) related to cognitive decline in a manner that could not be explained by Aβ and tau levels. We demonstrated that this SNP negatively affects cognitive function, partially through cortical thinning of the brain. In addition, through bioinformatics methods, we discovered that this SNP was associated with genes related to glutathione metabolism.

Although individuals with SNP showed similar AD pathologic burdens, they performed worse on cognitive function. To identify the underlying neurobiological substrates that lead to cognitive deterioration for the identified SNP, we performed SEM analysis. In the region-wide SEM analysis, we found that the SNP had a negative effect on cognitive performance partially through cortical thinning of the occipital and right posterior parietal cortices. The spatial pattern was different from that of CSF p-tau/$A\beta_{1\text{-}42}$, which involved wider cortical

areas, especially the medical temporal areas, which corresponds to AD signature regions implicated by previous studies.[32] Thus, the topologic difference in the effect of this SNP suggests a mechanistic process linking SNP, cortical thickness, and cognitive decline distinct from those of AD pathologies. In line with MRI findings, individuals with the SNP showed prominent cognitive deficit in the visuospatial domain, which is known to be processed in occipital and nondominant parietal cortices.[33]

The rs55906536 and 4 additional suggestive SNPs on chromosome 6 showed high linkage disequilibrium to each another. The MAF of the SNP was ≈8.0% to 9.5% (population including both Aβ positive and negative) across all datasets (ADNI-1, n = 136 and ADNI-GO/2, n = 658), which is in accordance with the previously reported prevalence of 8% for the European population.[34] This accordance indicates that the samples used in this study are not biased and may be representative of the whole White population.

Although the molecular mechanisms by which rs55906536 affects the cognitive decline in AD have not been validated, some possible explanations can be inferred from bioinformatics methods. By leveraging the 3D chromatin structure, we found that SNPs have physical interactions with the transcription start site of 15 genes (*TMEM14A*, *RPS16P5*, *MLIP-IT1*, *MIR5685*, *MCM3*, *LRRC1*, *GSTA7P*, *GSTA5*, *GSTA3*, *GSTA2*, *GFRAL*, *GCM1*, *FBXO9*, *FAM83B*, and *ELOVL5*) in the hippocampus and dorsolateral prefrontal cortex. The gene ontology analysis demonstrated that identified genes were enriched in 6 biological process and 1 molecular function. Among them, the glutathione-associated pathway was consistently identified, and we speculated that the glutathione pathway might mediate the SNPs to cognitive decline in AD.

Glutathione is a major endogenous enzyme-catalyzed antioxidant that plays a fundamental role in detoxification of reactive oxygen species (ROS) and regulates the intracellular redox environment.[35,36] Previous in vitro and in vivo studies have demonstrated a neuroprotective role of glutathione against oxidative insults; its deficiency in the brain leads to ROS-associated damage.[37–39] Glutathione reductions have been reported in animal models of AD[40] and patients with AD.[41,42] Our results suggest that individuals with the rs55906536 SNP might have a reduced or limited capacity to synthesize glutathione and are thus more vulnerable to ROS insult. To prove our speculation, we are planning to evaluate the levels of glutathione and oxidative stress markers in individuals with SNPs in the context of a future study.

Unlike rs55906536 and its linkage disequilibrium–linked SNPs, suggestive SNPs at chromosome 1 showed a protective effect against cognitive decline; individuals with SNPs at chromosome 1 showed higher cognitive functions with a similar level of AD pathologies. The gene expression analysis revealed that the minor allele of rs10889039 was associated with increased expression of the *DAB1* gene in brain tissues.

Disabled-1 (DAB1) protein is an essential component of the Reelin signal transduction pathway, which regulates synaptic neurotransmission, plasticity, and memory in the adult brain.[43] A number of studies have reported the protective role of Reelin and DAB1[44,45] by attenuating Aβ fibril formation and toxicity.[46,47] Consistent with previous studies, we showed that the SNP that is associated with increased expression of *DAB1* had a protective effect against cognitive decline.

This study has some limitations. First, this study was conducted with a data-driven approach. Furthermore, because we restricted the participants included to those with positive Aβ pathology, the sample size was small. However, replicated findings across various cognitive measures (MMSE, ADAS-cog, and MoCA) and across different datasets (ADNI-GO/2 and ADNI-1) strengthen the robustness of our findings. Nevertheless, our findings should be interpreted cautiously given the potential for false positives and replicated with a large data sample. Second, we measured Aβ and tau from the CSF data. Compared to CSF measures, Aβ and tau PET images can provide spatial information that can be used for more in-depth analysis. However, tau-PET (^{18}F-AV1451) is available for only a subset of participants in the ADNI dataset. Furthermore, while CSF Aβ and tau reflect the rates of both production and clearance at a given point in time,[48,49] Aβ and tau PET represent the magnitude of the neuropathologic load over time. Therefore, CSF Aβ and tau can be a better biomarker for a pathologic state. Third, it is known that a large number of individuals with AD have comorbid pathologies in addition to Aβ and tau accumulation.[50] Because we did not measure other AD-related pathologies such as transactive response DNA binding protein of 43 kDa and Lewy bodies, we were unable to evaluate whether unmeasured pathologies mediated the effect of the identified SNP on cognitive changes in AD.

Considering the highly complex multifactorial mechanisms of AD, it is important to identify the pathomechanisms that are common and distinct from typical AD pathogenesis. In this study, we identified SNPs related to cognitive function, which is not explained by the levels of Aβ and tau. Our findings support the growing literature on the role of glutathione in AD pathogenesis and may provide a new treatment strategy for AD such as antioxidative agents for individuals with the identified SNPs.

Acknowledgment

Data collection and sharing for this project were funded by the ADNI (NIH grant U01 AG024904) and Department of Defense ADNI (Department of Defense award W81XWH-12-2-0012). ADNI is funded by the National Institute on Aging, by the National Institute of Biomedical Imaging and Bioengineering, and through generous contributions from the following: AbbVie, Alzheimer's Association; Alzheimer's Drug Discovery Foundation; Araclon Biotech; BioClinica, Inc; Biogen; Bristol-Myers Squibb Co; CereSpir, Inc; Cogstate; Eisai Inc; Elan Pharmaceuticals, Inc; Eli Lilly and Co; EuroImmun; F. Hoffmann-La Roche Ltd and its affiliated company Genentech, Inc; Fujirebio; GE Healthcare; IXICO Ltd; Janssen Alzheimer

Immunotherapy Research & Development, LLC; Johnson & Johnson Pharmaceutical Research & Development LLC; Lumosity; Lundbeck; Merck & Co, Inc; Meso Scale Diagnostics, LLC; NeuroRx Research; Neurotrack Technologies; Novartis Pharmaceuticals Corp; Pfizer Inc; Piramal Imaging; Servier; Takeda Pharmaceutical Co; and Transition Therapeutics. The Canadian Institutes of Health Research is providing funds to support ADNI clinical sites in Canada. Private sector contributions are facilitated by the Foundation for the NIH (fnih.org). The grantee organization is the Northern California Institute for Research and Education, and the study is coordinated by the Alzheimer's Therapeutic Research Institute at the University of Southern California. ADNI data are disseminated by the Laboratory for Neuro Imaging at the University of Southern California.

Study funding

This research was supported by Korea Health Technology Research and Development Project through the Korea Health Industry Development Institute, funded by the Ministry of Health & Welfare, Republic of Korea (HI14C2768). This research was supported by the Brain Research Program through the National Research Foundation of Korea funded by the Ministry of Science and Information & Communication Technology, Republic of Korea (2016M3C7A1913844). This research was supported by the Bio & Medical Technology Development Program through the National Research Foundation of Korea funded by the Ministry of Science and Information & Communication Technology, Republic of Korea (2016941946).

Disclosure

The authors report no disclosures relevant to the manuscript. Go to Neurology.org/N for full disclosures.

Publication history

Received by *Neurology* July 31, 2019. Accepted in final form April 27, 2020.

Appendix Authors

Name	Location	Contribution
Hang-Rai Kim, MD	Korea Advanced Institute of Science and Technology, Daejeon	Design and conceptualized study; collected and analyzed the data; drafted the manuscript for intellectual content; performed statistical analysis
Taeyeop Lee, MD	Korea Advanced Institute of Science and Technology, Daejeon	Collected and analyzed the data
Jung Kyoon Choi, PhD	Korea Advanced Institute of Science and Technology, Daejeon	Interpreted the data; revised the manuscript for intellectual content
Yong Jeong, MD	Korea Advanced Institute of Science and Technology, Daejeon	Design and conceptualized study; revised the manuscript for intellectual content

References

1. Price DL, Tanzi RE, Borchelt DR, Sisodia SS. Alzheimer's disease: genetic studies and transgenic models. Annu Rev Genet 1998;32:461–493.
2. Hardy J, Selkoe DJ. The amyloid hypothesis of Alzheimer's disease: progress and problems on the road to therapeutics. Science 2002;297:353–356.
3. Pimplikar SW. Reassessing the amyloid cascade hypothesis of Alzheimer's disease. Int J Biochem Cell Biol 2009;41:1261–1268.
4. Morris GP, Clark IA, Vissel B. Questions concerning the role of amyloid-β in the definition, aetiology and diagnosis of Alzheimer's disease. Acta Neuropathol 2018;136:663–689.
5. Bennett DA, Schneider JA, Arvanitakis Z, et al. Neuropathology of older persons without cognitive impairment from two community-based studies. Neurology 2006;66:1837–1844.
6. Mintun M, Larossa G, Sheline Y, et al. [^{11}C] PIB in a nondemented population: potential antecedent marker of Alzheimer disease. Neurology 2006;67:446–452.
7. Giannakopoulos P, Herrmann FR, Bussière T, et al. Tangle and neuron numbers, but not amyloid load, predict cognitive status in Alzheimer's disease. Neurology 2003;60:1495–1500.
8. Driscoll I, Troncoso J. Asymptomatic Alzheimer's disease: a prodrome or a state of resilience? Curr Alzheimer Res 2011;8:330–335.
9. Hardy J, De Strooper B. Alzheimer's disease: where next for anti-amyloid therapies? Brain 2017;140:853–855.
10. Hyman BT. Amyloid-dependent and amyloid-independent stages of Alzheimer disease. Arch Neurol 2011;68:1062–1064.
11. Pimplikar SW, Nixon RA, Robakis NK, Shen J, Tsai LH. Amyloid-independent mechanisms in Alzheimer's disease pathogenesis. J Neurosci 2010;30:14946–14954.
12. Lambert JC, Ibrahim-Verbaas CA, Harold D, et al. Meta-analysis of 74,046 individuals identifies 11 new susceptibility loci for Alzheimer's disease. Nat Genet 2013;45:1452–1458.
13. Shaw LM, Vanderstichele H, Knapik-Czajka M, et al. Cerebrospinal fluid biomarker signature in Alzheimer's Disease Neuroimaging Initiative subjects. Ann Neurol 2009;65:403–413.
14. Purcell S, Neale B, Todd-Brown K, et al. PLINK: a tool set for whole-genome association and population-based linkage analyses. Am J Hum Genet 2007;81:559–575.
15. Fuchsberger C, Abecasis GR, Hinds DA. Minimac2: faster genotype imputation. Bioinformatics 2014;31:782–784.
16. Howie B, Fuchsberger C, Stephens M, Marchini J, Abecasis GR. Fast and accurate genotype imputation in genome-wide association studies through pre-phasing. Nat Genet 2012;44:955–959.
17. Desikan RS, Ségonne F, Fischl B, et al. An automated labeling system for subdividing the human cerebral cortex on MRI scans into gyral based regions of interest. Neuroimage 2006;31:968–980.
18. Wang L, Benzinger TL, Hassenstab J, et al. Spatially distinct atrophy is linked to β-amyloid and tau in preclinical Alzheimer disease. Neurology 2015;84:1254–1260.
19. De Jong D, Jansen RW, Kremer BP, Verbeek MM. Cerebrospinal fluid amyloid β42/phosphorylated tau ratio discriminates between Alzheimer's disease and vascular dementia. J Gerontol A Biol Sci Med Sci 2006;61:755–758.
20. Maddalena A, Papassotiropoulos A, Müller-Tillmanns B, et al. Biochemical diagnosis of Alzheimer disease by measuring the cerebrospinal fluid ratio of phosphorylated tau protein to β-amyloid peptide42. Arch Neurol 2003;60:1202–1206.
21. Stranger BE, Stahl EA, Raj T. Progress and promise of genome-wide association studies for human complex trait genetics. Genetics 2011;187:367–383.
22. Devlin B, Roeder K, Wasserman L. Genomic control, a new approach to genetic-based association studies. Theor Popul Biol 2001;60:155–166.
23. Nasreddine ZS, Phillips NA, Bédirian V, et al. The Montreal Cognitive Assessment, MoCA: a brief screening tool for mild cognitive impairment. J Am Geriatr Soc 2005;53:695–699.
24. Jack CR, Knopman DS, Jagust WJ, et al. Tracking pathophysiological processes in Alzheimer's disease: an updated hypothetical model of dynamic biomarkers. Lancet Neurol 2013;12:207–216.
25. Bentler PM. Comparative fit indexes in structural models. Psychol Bull 1990;107:238–246.
26. Hu Lt, Bentler PM. Cutoff criteria for fit indexes in covariance structure analysis: conventional criteria versus new alternatives. Struct Equation Model 1999;6:1–55.
27. Arbuckle JL, Wothke W. Amos 4.0 User's Guide. Chicago: SmallWaters Corp; 1999.
28. Yang D, Jang I, Choi J, et al. 3DIV: a 3D-genome interaction viewer and database. Nucleic Acids Res 2017;46:D52–D57.
29. Chen EY, Tan CM, Kou Y, et al. Enrichr: interactive and collaborative HTML5 gene list enrichment analysis tool. BMC Bioinformatics 2013;14:128.
30. Lonsdale J, Thomas J, Salvatore M, et al. The Genotype-Tissue Expression (GTEx) project. Nat Genet 2013;45:580.
31. Connor DJ, Sabbagh MN. Administration and scoring variance on the ADAS-Cog. J Alzheimers Dis 2008;15:461–464.
32. Braak H, Braak E. Neuropathological stageing of Alzheimer-related changes. Acta Neuropathol 1991;82:239–259.
33. Colby CL, Goldberg ME. Space and attention in parietal cortex. Annu Rev Neurosci 1999;22:319–349.
34. Sherry ST, Ward MH, Kholodov M, et al. dbSNP: the NCBI database of genetic variation. Nucleic Acids Res 2001;29:308–311.
35. Hammond CL, Lee TK, Ballatori N. Novel roles for glutathione in gene expression, cell death, and membrane transport of organic solutes. J Hepatol 2001;34:946–954.

36. Dringen R. Metabolism and functions of glutathione in brain. Prog Neurobiol 2000; 62:649–671.
37. Jain A, Mårtensson J, Stole E, Auld PA, Meister A. Glutathione deficiency leads to mitochondrial damage in brain. Proc Natl Acad Sci USA 1991;88:1913–1917.
38. Mytilineou C, Kramer BC, Yabut JA. Glutathione depletion and oxidative stress. Parkinsonism Relat Disord 2002;8:385–387.
39. Wüllner U, Löschmann P-A, Schulz JB, et al. Glutathione depletion potentiates MPTP and MPP+ toxicity in nigral dopaminergic neurones. Neuroreport 1996;7:921–923.
40. Resende R, Moreira PI, Proença T, et al. Brain oxidative stress in a triple-transgenic mouse model of Alzheimer disease. Free Radic Biol Med 2008;44:2051–2057.
41. Lovell MA, Xie C, Markesbery WR. Decreased glutathione transferase activity in brain and ventricular fluid in Alzheimer's disease. Neurology 1998;51:1562–1566.
42. Mandal PK, Tripathi M, Sugunan S. Brain oxidative stress: detection and mapping of anti-oxidant marker "glutathione" in different brain regions of healthy male/female, MCI and Alzheimer patients using non-invasive magnetic resonance spectroscopy. Biochem Biophys Res Commun 2012;417:43–48.
43. Förster E, Bock HH, Herz J, Chai X, Frotscher M, Zhao S. Emerging topics in Reelin function. Eur J Neurosci 2010;31:1511–1518.
44. Gao H, Tao Y, He Q, Song F, Saffen D. Functional enrichment analysis of three Alzheimer's disease genome-wide association studies identities DAB1 as a novel candidate liability/protective gene. Biochem Biophys Res Commun 2015;463: 490–495.
45. Cuchillo-Ibañez I, et al. The β-amyloid peptide compromises Reelin signaling in Alzheimer's disease. Sci Rep 2016;6:31646.
46. Pujadas L, Rossi D, Andrés R, et al. Reelin delays amyloid-beta fibril formation and rescues cognitive deficits in a model of Alzheimer's disease. Nat Commun 2014;5:3443.
47. Lane-Donovan C, Philips GT, Wasser CR, et al. Reelin protects against amyloid β toxicity in vivo. Sci Signal 2015;8:384.
48. Blennow K, Hampel H. CSF markers for incipient Alzheimer's disease. Lancet Neurol 2003;2:605–613.
49. Gordon BA, Friedrichsen K, Brier M, et al. The relationship between cerebrospinal fluid markers of Alzheimer pathology and positron emission tomography tau imaging. Brain 2016;139:2249–2260.
50. Rabinovici GD, Carrillo MC, Forman M, et al. Multiple comorbid neuropathologies in the setting of Alzheimer's disease neuropathology and implications for drug development. Alzheimers Dement 2016;3:83–91.